Organic & Biomolecular Chemistry

PAPER

View Article Online
View Journal | View Issue

Cite this: *Org. Biomol. Chem.*, 2016, **14**, 1680

Tandem buildup of complexity of aromatic molecules through multiple successive electrophile generation in one pot, controlled by varying the reaction temperature†

Akinari Sumita, Yuko Otani and Tomohiko Ohwada*

Received 30th October 2015,
Accepted 16th December 2015

DOI: 10.1039/c5ob02240a

www.rsc.org/obc

While some sequential electrophilic aromatic substitution reactions, known as tandem/domino/cascade reactions, have been reported for the construction of aromatic single skeletons, one of the most interesting and challenging possibilities remains the one-pot build-up of a complex aromatic molecule from multiple starting components, *i.e.*, ultimately multi-component electrophilic aromatic substitution reactions. In this work, we show how tuning of the leaving group ability of phenolate derivatives from carbamates and esters provides a way to successively generate multiple unmasked electrophiles in a controlled manner in one pot, simply by varying the temperature. Here, we demonstrate the autonomous formation of up to three bonds in one pot and formation of two bonds arising from a three-component electrophilic aromatic substitution reaction. This result provides a proof-of-concept of our strategy applicable for the self-directed construction of complex aromatic structures from multiple simple molecules, which can be a potential avenue to realize multi-component electrophilic aromatic substitution reactions.

Introduction

The assembly of multiple functionalized aromatic structures into a single molecule is of interest in drug design, as exemplified by the integration of multiple functionalized aromatic pharmacophores.[1] For this purpose, the idea of sequentially connecting structurally simple aromatic compounds seems to be an attractive approach.[2] Electrophilic aromatic substitution (S_EAr) reactions can be used for individual functionalization of several different aromatic moieties in a single molecule (Chart 1). The conventional methodology would be convergent connection of several substituted aromatic compounds through electrophilic centers, as shown in Chart 1(a). However, this approach often requires workup/isolation processes to minimize side reactions or to remove excess reactants or by-products. For example, the reactivity of electrophiles is frequently insufficient to drive the reaction to completion, so an excess amount of aromatic compound(s) is often used to promote the intermolecular S_EAr reaction (*vide infra*). On the other hand, one of the most interesting and challenging possibilities is one-pot build-up of a complex aromatic molecule from multiple starting components, *i.e.*, ultimately multi-component electrophilic aromatic substitution reactions (Chart 1(b)). This strategy requires precise temporal control of bond formation *via* multiple sequential electrophilic aromatic substitution reactions in order to increase molecular complexity in a precisely defined manner. Several sequential electrophilic aromatic substitution reactions, known as tandem/domino/cascade reactions, have already been reported for the construction of aromatic single skeletons such as indoles,[3] indenes,[4] dihydroindenes,[5] indanones,[6] fluorenes,[7] carbazoles,[8] di- and triphenylmethane,[9] naphthoquinones,[10] and other skeletons.[11] However, most of these reactions are limited to only two kinds of reactions, *i.e.*, involving the formation of two bonds, often *via* intermolecular–intramolecular or intramolecular–intermolecular sequences (Chart 1(c)). The main reason for this is that most of the reactions require the use of an excess amount of aromatic compound(s) to effectively promote the intermolecular S_EAr reaction, and thus the following S_EAr reaction is inevitably restricted to a kinetically favorable intramolecular reaction (Chart 1(c-1)), or *vice versa* (Chart 1(c-2)). Low reactivity of electrophiles is also a reason why many electrophilic reactions are unsuitable for multi-component electrophilic aromatic substitution reactions: specifically, the second S_EAr reaction can start before the first S_EAr reaction is completed, and therefore the chemoselectivity is impaired. Thus, current methodology in this field is commonly restricted to the formation of two bonds, of which one is intramolecular.

Graduate School of Pharmaceutical Sciences, The University of Tokyo, 7-3-1 Hongo, Bunkyo-ku, Tokyo 113-0033, Japan. E-mail: ohwada@mol.f.u-toko.ac.jp

†Electronic supplementary information (ESI) available: Full experimental sections, details of computation, and ^1H and ^{13}C NMR spectra. See DOI: 10.1039/c5ob02240a

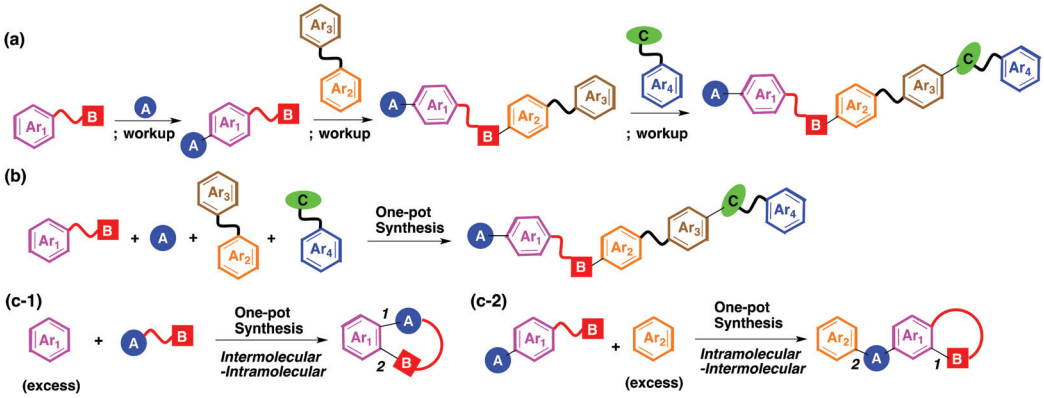

Chart 1 (a) Conventional step-by-step build-up of aromatic molecules through electrophilic substitution. (b) Hypothetical multi-component aromatic electrophilic reactions in one pot. (c-1/c-2) Previous examples of two-step tandem reactions.

One way to achieve multi-component electrophilic aromatic substitution reactions would be precise temporal control of the generation of highly reactive electrophiles, which can react rapidly with the target aromatic compound even when the target aromatic compound is present only in a stoichiometric amount.

An approach to the generation of such electrophiles has been to transform masked (deactivated or latent) electrophiles into active (unmasked) electrophiles. For example, ureas and carbamates can be regarded as masked isocyanate cations that can be activated *via* N–C and O–C bond cleavage.[12] There have been a few reports on the application of masked isocyanate cations to S_EAr reactions.[12f–h] These S_EAr reactions of masked isocyanate cations have been used for intramolecular reactions, such as the construction of dihydroisoquinolones[12g,h] or isoindolin-1-one,[12f,g] but they are not suitable for intermolecular S_EAr reactions due to the moderate yields, requirement of excess amounts of aromatic compounds, and the need for heating. These are obstacles for application in tandem/cascade/domino reactions. To our knowledge, there are few reports of sequential multiple unmasking reactions, mainly because the unmasking reaction rate is usually dependent on the substrate structure, not on the leaving group, resulting in severe limitations on suitable reactants.[13a] Thus, for the development of multi-component S_EAr reactions, new chemical species of leaving groups are required, which can control the unmasking reaction rates.

In this paper, we report successive reaction-temperature-controlled generation of multiple unmasked electrophiles, particularly isocyanate cations and related cations, leading to autonomous sequential electrophilic aromatic substitution reactions. To achieve this, we focused on control of the bond strength of the leaving groups in carbamates as a strategy to obtain the differential leaving ability in order to control the generation of multiple electrophiles. We demonstrated autonomous formation of up to three bonds in one pot and the formation of two bonds arising from a three-component electrophilic aromatic substitution reaction. The present study provides a proof-of-concept of our strategy applicable for the self-directed construction of complex aromatic structures from multiple simple molecules, which can be a potential avenue to realize multi-component electrophilic aromatic substitution reactions, as illustrated in Chart 1(b).

Results and discussion

Tuning of leaving groups in aromatic amidation and acylation

We recently have shown that methyl salicylate is a good leaving group from carbamate (which is a stable functional group) under relatively strong acid-catalyzed conditions.[13] The methyl ester group, located at the *ortho* position with respect to the phenolic oxygen atom, assists partial protonation of, or H-bonding to, the phenolic oxygen atom, which weakens the C–O (phenolic) bond, resulting in ready C–O bond cleavage to generate isocyanate cations at 20 °C (20 °C for 90 minutes: **1b**, Fig. 1(a)).[14] We have demonstrated previously that *N*-H and *N*-alkyl or *N*-aryl isocyanate cations show different reactivities: *N*-alkyl and *N*-aryl isocyanate cations are generated from the carbamates more slowly than *N*-H isocyanate cations.[13a] While multiple amidations can be achieved by using isocyanate cations with different reactivities, we found here that tuning of the leaving group ability to generate the isocyanate cations is a more effective strategy to achieve multiple amidations.

Indeed, we found that when the ester group is substituted at the *para*-position with respect to the phenolic oxygen atom (**1a**, Fig. 1(a)), C–O (phenolic) bond cleavage occurs slowly even on heating (at 40 °C, 26 hours). Therefore, the change in the reaction temperature can be used to control the time of generation of even the same reactive electrophile, the isocyanate cation.

Because the substitution position of the ester groups dramatically changes the C–O bond cleavage reaction rates of carbamates bearing methyl salicylates, we expected that adding another ester group into the leaving group (methyl salicylate) would increase the unmasking reaction rate. It turned out that dimethyl 4-hydroxyisophthalate (**1d**), containing two ester

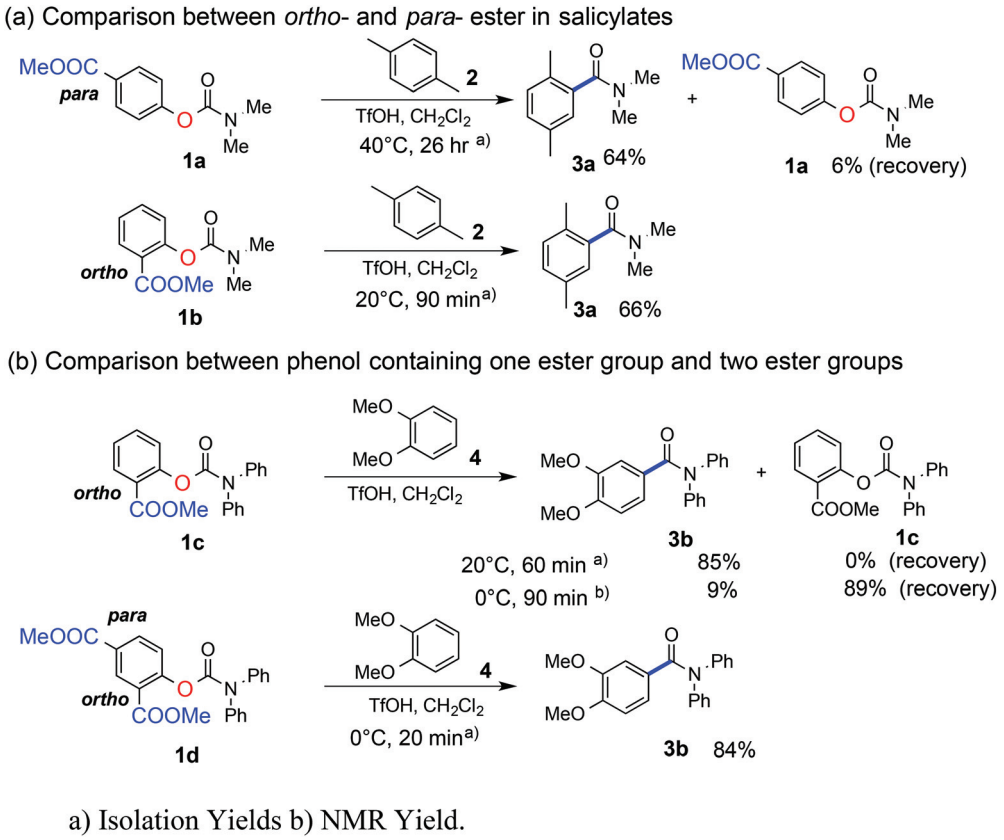

Fig. 1 Control of amide formation based on different leaving abilities.

groups at the *ortho*- and *para*-positions with respect to the phenolic oxygen atom, is a better leaving group than methyl salicylate (**1c**). In the case of **1d**, the leaving group is cleaved to form isocyanate cations even at 0 °C, and the reaction is completed within 20 minutes (Fig. 1(b)). Thus, at 0 °C, the reaction of methyl salicylate (**1c**) can be differentiated from the reaction of diester **1d**.

This concept is also applicable to differentiate between esters and carbamates, that is, between the generation of acyl cations and isocyanate cations. Because the C–O bond strength in esters **1e** is weaker than that in carbamates **1c**, the C–O bond in esters is cleaved faster than the C–O bond in carbamates: this enables temperature control of the generation of acyl cations (at 0 °C) and isocyanate cations (at 20 °C) (Fig. 2). Thus,

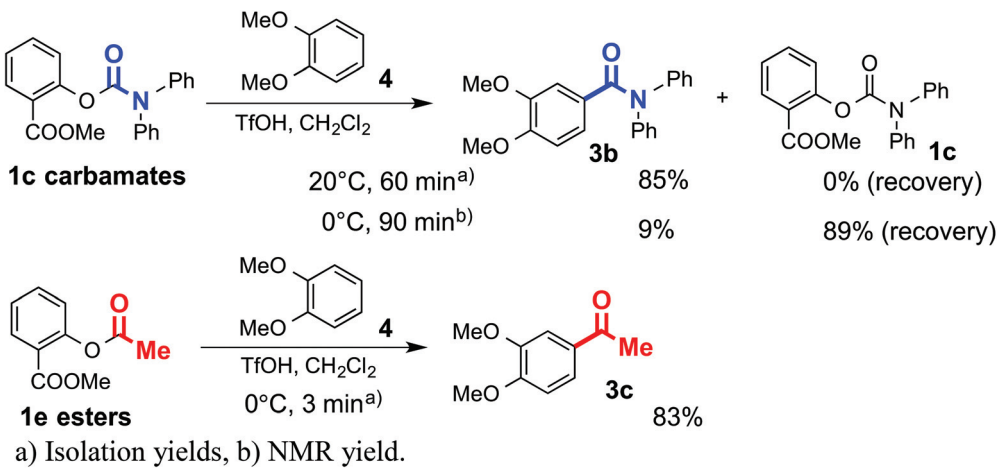

Fig. 2 Comparison of amide formation rate and ketone formation rate.

we can control the speed of unmasking to generate different reactive electrophiles simply by changing the temperature.

Activation of leaving groups through protonation and hydrogen bonding

We conducted kinetic studies to characterize the difference in the leaving ability between the monoester leaving group (see **1b**) and diester leaving group (see **1f**). Fig. 3 shows the dependence of the reaction profiles on the acidity of the medium. In the case of monoester leaving group (**1b**), as the acidity is increased, the reaction rate increases to a broad maximum, and then decreases in the strong acidity region. *O*,*O*-Diprotonation of salicyl carbamates (like **TS-1b′**, Fig. 3a) can be observed by proton NMR spectroscopy in a strong acid ($-H_0$ = 14). Cleavage of the C–O bond of the diprotonated species will be difficult because of the generation of one neutral species (methyl salicylate) and one rather unstable dicationic species (*O*-protonated carbamate dication). Therefore, this means that the monocationic species (**TS-1b**, Fig. 3a) rather than the diprotonated species (**TS-1b′**, Fig. 3a) is involved in the bond dissociation transition state.[13]

On the other hand, in the case of the diester leaving group (**1f**), as the acidity increased, the reaction rate increases monotonically to a broad maximum from a relatively weak acidic region ($-H_0$ = 10) to a strong acidic region ($-H_0$ = 14) (Fig. 3b). Because the *ortho*-monoester-substituted carbamate (**1b**) is diprotonated in the strong acidic region ($-H_0$ = 14) (see **TS-1b′**, Fig. 3a), disubstituted carbamate (**1f**) also can be diprotonated in the strong acidic region ($-H_0$ = 14). When the carbonyl oxygen atom of the carbamate functional group of diester-substituted carbamate (**1f**) is protonated (**TS-1f′**, Fig. 3), the C–O bond cleavage of this diprotonated species will be difficult because of the generation of one neutral species and one rather unstable gitonic (close) dicationic isocyanate cation species. Therefore, the C–O bond cleavage of the diprotonated species will take place through the alternative diprotonated state **TS-1f** rather than the dication state **TS-1f′** (Fig. 3).

Computational support for leaving group activation

These kinetic results are supported by the results of calculations (Fig. 4). The calculated energy differences are shown in terms of $\Delta\Delta G$ at 25 °C (298 K), together with $\Delta\Delta H$.

In the continuum environment of TfOH, there are several possible stable conformers of diester-substituted carbamate **1f** in protonated states, because the diester carbamate functionalities have several basic sites.[13a,b] The ester carbonyl oxygen atom(s), the most basic sites, is mono-protonated or are di-protonated, such cationic species, **1f-SM$_0$-H$^+$** and **1f-SM$_0$-2H$^+$**, are

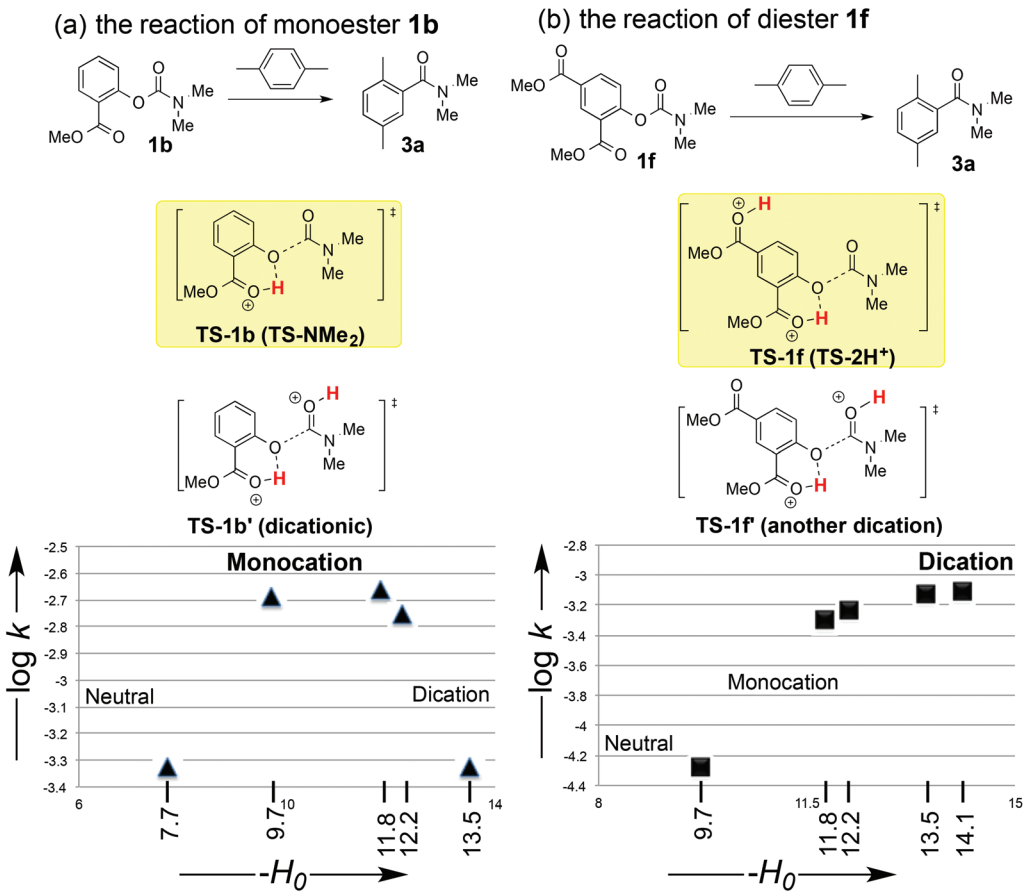

Fig. 3 Acidity-dependence of the reaction profiles of different leaving groups (measured at 31 °C for (a), and at −6 °C for (b)).

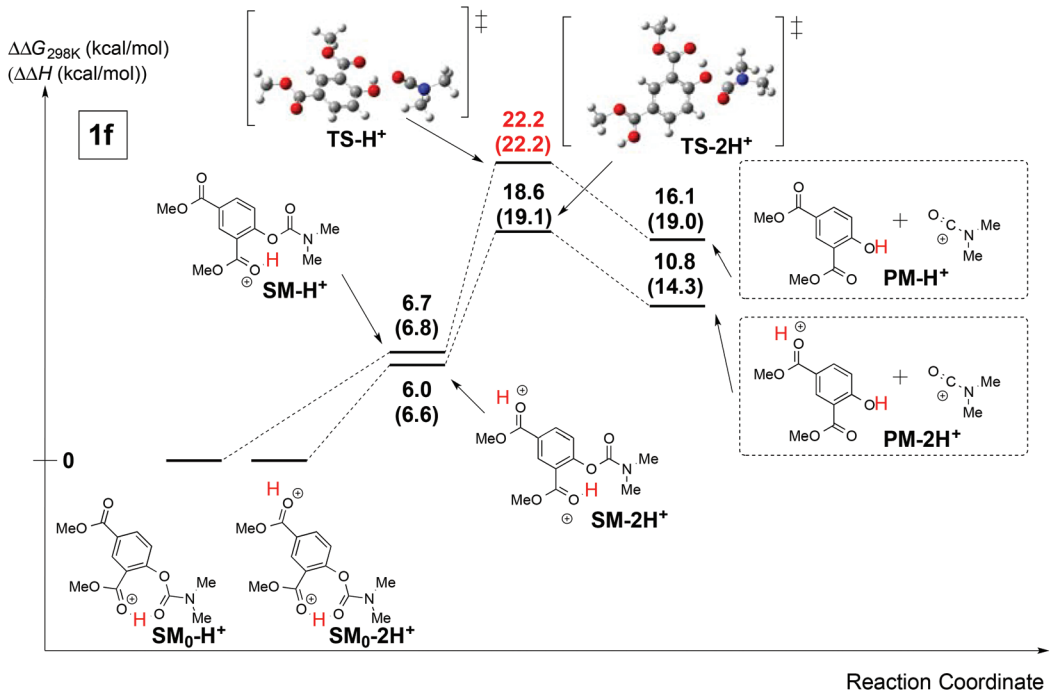

Fig. 4 Calculated energy diagram of C–O bond cleavage steps of **1f** (CPCM-M06-2X/6-311++G(d,p)//CPCM-B3LYP/6-31+G(d)).

the most stable (Fig. 4). On the other hand, a proton can switch the protonation site to the less basic phenolic oxygen atom, and such isomeric conformers, **1f-SM-H**$^+$ and **1f-SM-2H**$^+$, are destabilized as compared to the most stable conformers (**1f-SM$_0$-H**$^+$, **1f-SM$_0$-2H**$^+$). Destabilization is similar in magnitude in both cases of the monocation and the dication, and the energy gaps are attainable probably because of the formation of intramolecular hydrogen bonding. Through the intervention of these equilibrating species, **1f-SM-H**$^+$ and **1f-SM-2H**$^+$, the transition states of C–O bond dissociation can be obtained (Fig. 4): the activation energy from the most stable conformer **1f-SM$_0$-2H**$^+$ through the dicationic state (**1f-TS-2H**$^+$) ($\Delta\Delta G_{298\ K}$: 18.6 kcal mol^{-1}; $\Delta\Delta H$: 19.1 kcal mol^{-1}) is lower than that from **1f-SM$_0$-H**$^+$ through the monocationic state (**1f-TS-H**$^+$) ($\Delta\Delta G_{298\ K}$: 22.2 kcal mol^{-1}; $\Delta\Delta H$: 22.2 kcal mol^{-1}). Other calculation levels (M06, M06-HF, B3LYP, B3PW91, MP2) also converged to similar results (ESI, Fig. SI1 and 2†). Thus, the observed acidity–rate relationship (Fig. 3) can be rationally explained. Moreover, the difference in energy between the dicationic pathway and monocationic pathway amounts to 3 kcal mol^{-1}, which means that the reaction pathway of C–O bond dissociation through the dicationic state should be dominant.

The reaction rate of ester (**1e**) could not be measured due to the very rapid unmasking rate; however, the calculation results support a marked difference in reaction rates between the relevant carbamate and ester (Fig. 5). From the calculation result, the activation energy of C–O bond cleavage of the monoester-substituted carbamate **1b** from the most stable conformer (**SM$_0$-1b**) through the equilibrating minor monocationic species (**SM-1b**), $\Delta\Delta G_{298\ K}$: 23.0 kcal mol^{-1}; $\Delta\Delta H$: 24.5 kcal mol^{-1}, is higher than that of C–O bond cleavage of the ester from the more stable monocationic species (**SM-1e**), $\Delta\Delta G_{298\ K}$: 13.1 kcal mol^{-1}; $\Delta\Delta H$: 13.7 kcal mol^{-1}. This may be partially true because the carbamate is more stable than the ester due to Y-type conjugation,[12h,15] and thus more energy is needed to break the stable C–O bond of the carbamate. In the case of ester, it is worth noting that when the intramolecular hydrogen bond is formed with the phenolic oxygen atom, the conformer **SM-1e** is more stable than the isomeric **SM$_0$-1e** (Fig. 5). Therefore, an ester compound bearing the methyl salicylester group can easily cleave its O–C bond. These calculations are consistent with the experimental results: the reaction of ester (**1e**) is dramatically faster than that of monoester-substituted carbamate **1b**, and **1e** is distinctly faster than the diester-substituted carbamate **1f**. Other calculation levels (M06, MP2) also support this conclusion (ESI, Fig. SI3 and 4†) and the observed relationship (Fig. 2).

Temperature control of multiple electrophile generation, enabling two-step buildup of complexity of aromatic molecules

Based on the above findings, we considered that temperature control for unmasking electrophiles could be applied to build-up aromatic molecular complexity in one-pot reactions (Fig. 6–8 and Tables 1 and 2). First, we explored the formation of two bonds.

Double aromatic amidations

Fig. 6 shows a representative example of the build-up of two kinds of aromatic amide molecules. Mixing **4** and **5** in the

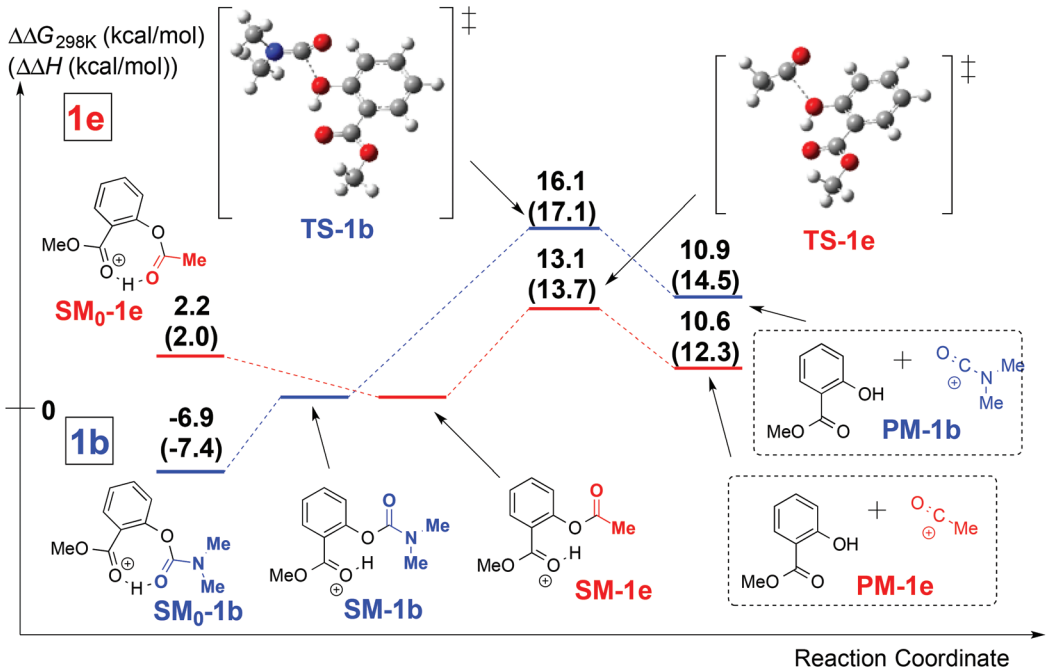

Fig. 5 Calculated energy diagrams of C–O bond cleavage steps of **1b** and **1e** (CPCM-M06-2X/6-311++G(d,p)//CPCM-B3LYP/6-31+G(d)).

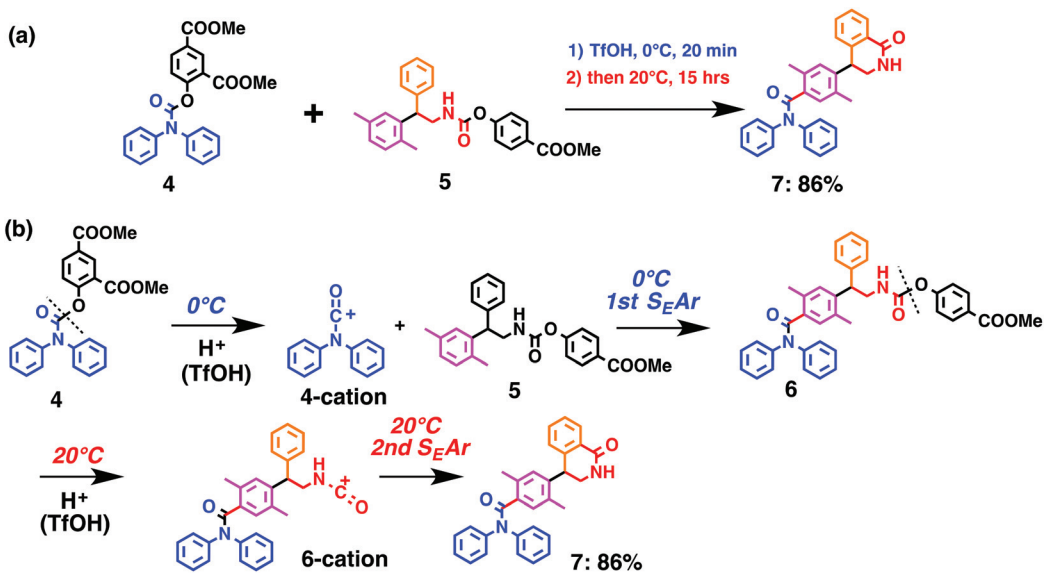

Fig. 6 Formation of two amide bonds through temperature-controlled multiple electrophile generation: (a) overall reaction (b) individual steps.

presence of TfOH produced compound 7 in 86% yield (Fig. 6(a), in which the reaction temperature was changed from 0 °C to 20 °C). First, the corresponding isocyanate cation (**4-cation**) was generated from carbamate bearing *ortho*, *para*-disubstituted phenol at 0 °C, and then the electron-rich aromatic ring (magenta) of **5** reacted with the resulting isocyanate cation (blue) to form a C–C bond in the aromatic amide structure **6** (red bond) (Fig. 6(b)). Under cooling (0 °C), the carbamate containing *para*-monosubstituted phenol did not uncage to form the isocyanate cation (**4-cation**). When the reaction mixture was warmed to room temperature (20 °C), the second isocyanate cation (**6-cation**, red) was generated from the carbamate containing *para*-monosubstituted phenol (**6**), and the second aromatic compound (orange) reacted with the isocyanate cation

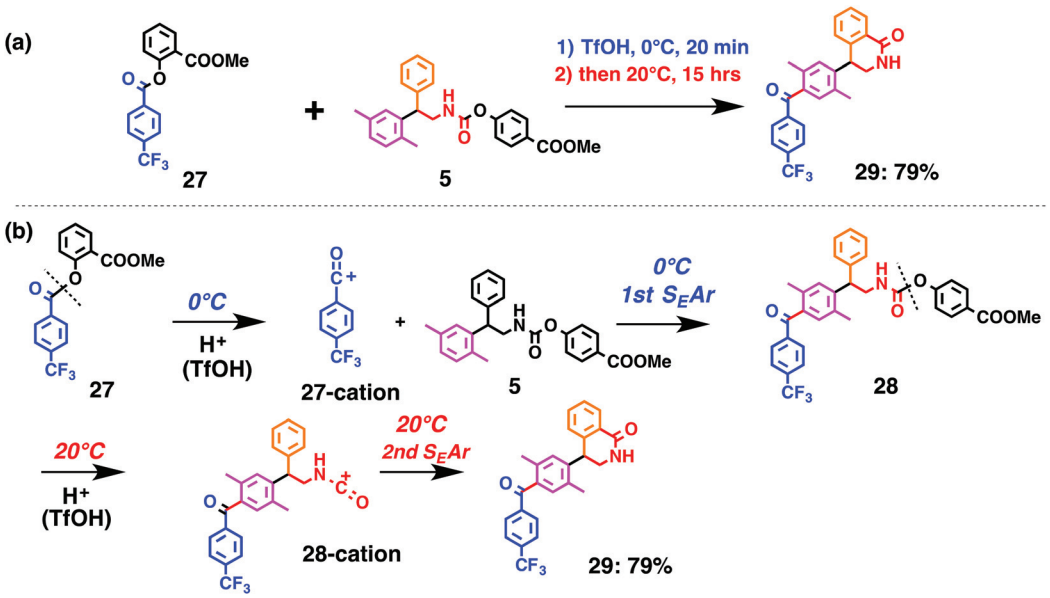

Fig. 7 Ketone and amide bond formations through temperature control of multiple electrophile generation: (a) overall reaction (b) individual steps.

(**6-cation**) to form a C–C bond in the aromatic amide structure, affording **7** in an intramolecular manner in this example (red bond) (Fig. 6(b)). The yield that is shown is over the two steps; thus, the average yield of each reaction is larger than 93%.

The generality of this sequential dual amidation reaction was examined and the results are shown in Table 1, which supports the feasibility of multiple intermolecular or intramolecular amidation reactions. Because the reaction temperature (20 °C) is not so high, ethyl carbamate (**8**),[12h] the ester groups (**14** and **16**),[16] and a methoxy group (**15**)[17] can be tolerated; the former substituents can generate electrophile species, and the latter substituent can be demethylated. Examples of successive double intermolecular reactions were also obtained (entries 4 and 5, Table 1). After the first S_EAr reaction was completed (the formation of **16** or **20**), one aromatic molecule (**17** or **21**) was added and the reaction mixture was warmed to 20 °C to produce a double amidation product (**18** and **22**), respectively. Importantly, a three-component reaction to create two amide bonds can be realized (entry 6, Table 1): when TfOH was added into a mixture of three components (**14**, **23**, **26**) at 0 °C and then at 20 °C, the product **25** was obtained, though in moderate yield (overall yield for the two step reaction is 48%). One of the (equivalent) aromatic rings of the substrate **23** can react with the first electrophile (generated at 0 °C from **14**), leading to the intermediate **24** smoothly, because we used stoichiometric amounts of the aromatic substrate (**23**) and the electrophile (**14**), to minimize side reactions. Then, the intermediate **24** reacted with the second electrophile, generated from **26** at 20 °C, to give compound **25**. This result demonstrates that the strategy of tuning the leaving group ability of masked electrophiles, *e.g.*, the phenolate derivatives, should be valid for real multi-component electrophilic aromatic substitution reactions. The average yield of each reaction ranged from 60% to 93% (Table 1).

Sequential aromatic acylation-amidation

Fig. 7 shows a representative example of one-pot build-up of aromatic ketone and aromatic amide molecules. Mixing **27** and **5** in the presence of TfOH produced compound **29** in 79% yield, by the change in the reaction temperature from 0 °C to 20 °C (Fig. 7(a)). First, the corresponding acyl cation (**27-cation**) was generated from the carbamate bearing *ortho*-substituted phenol at 0 °C, and then the electron-rich aromatic ring (magenta) of **5** reacted with the resulting acyl cation (blue) to form a C–C bond in the aromatic ketone structure **28** (red bond; Fig. 7(b)). At 0 °C, the carbamate containing *para*-monosubstituted phenol did not decompose to isocyanate cation. However, on warming the reaction mixture to room temperature (20 °C), the second isocyanate cation (**28-cation**, red) was generated from the carbamate containing *para*-monosubstituted phenol (**28**), and the second aromatic compound (orange) reacted with the resulting isocyanate cation (**28-cation**) in an intramolecular manner to form an aromatic amide bond (red bond in product **29**) (Fig. 7(b)). Again the yield shown is the two-step yield, and the average yield of each reaction was larger than 89%.

The generality of this sequential acylation–amidation reaction was examined and the results are shown in Table 2, which supports the feasibility of multiple intermolecular or intramolecular acylation–amidation reactions. Substrates bearing a trifluoromethyl group (**27**)[18] or an ester group (**30**)[15] can produce electrophile species, but because of the low temperature (0 °C to 20 °C), acylation–amidation reactions are accomplished without interference from these functional groups. After the first S_EAr reaction was completed (the formation of **36** or **39**), the aromatic substrate (**37** or **40**)

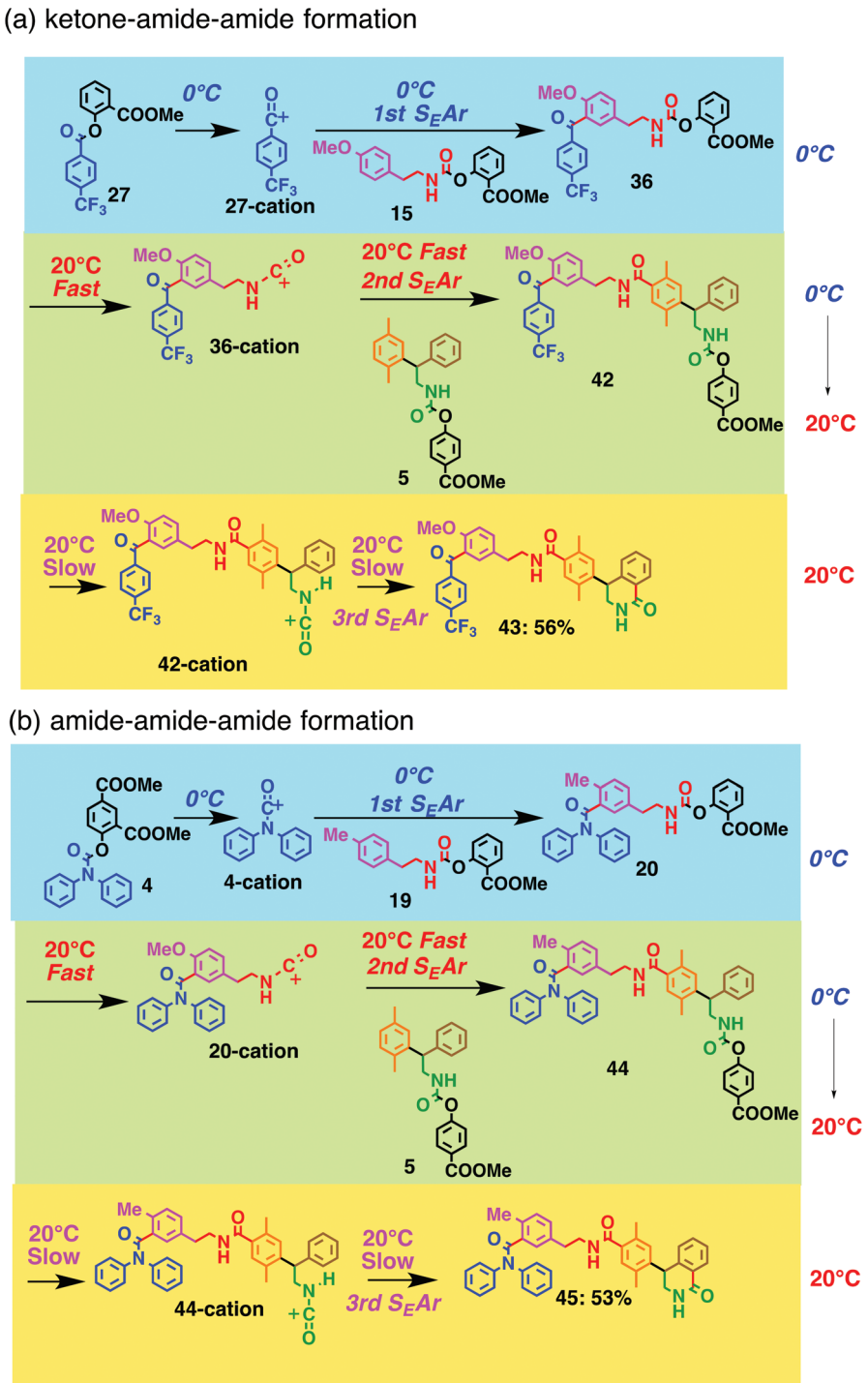

Fig. 8 Temperature control of multiple electrophile generation, enabling three-step buildup of complexity of aromatic molecules ((a) ketone–amide–amide; (b) amide–amide–amide).

was added, and therefore three kinds of starting materials are combined sequentially into a single aromatic molecule (**38** or **41**) in one pot. The average yield of each reaction ranged from 77% to 89%.

Formation of three bonds in a one-pot reaction

Finally, we demonstrate the formation of three inter- and intramolecular bonds constituting ketone/amide functionalities in one pot (Fig. 8). The first electrophiles (blue) are generated from ester (**27**) containing *ortho*-mono-substituted phenol (methyl salicylate) (Fig. 8(a)) or carbamate (**4**) (Fig. 8(b)) containing *ortho*, *para*-disubstituted phenol at 0 °C, followed by generation of the second electrophiles (red) from carbamate (**36** or **20**) containing *ortho*-monosubstituted phenol at 20 °C for around 30 min. The third electrophiles (green) are gener-

Table 1 Two-step buildup of complexity of aromatic molecules by dual amidation

Entry	Substrates	Reaction temperature 1	Intermediate	Reaction temperature 2 and 3rd substrate	Final product
1	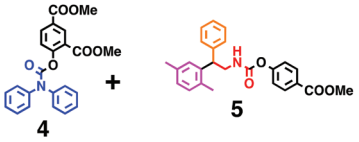	0 °C	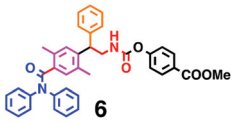	20 °C	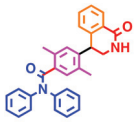 7: 86%
2	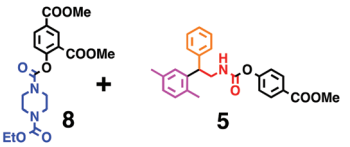	0 °C	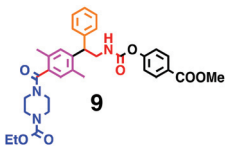	20 °C	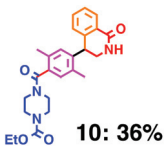 10: 36%
3	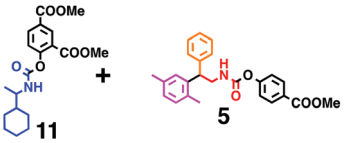	0 °C	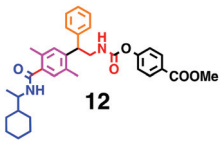	20 °C	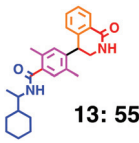 13: 55%
4	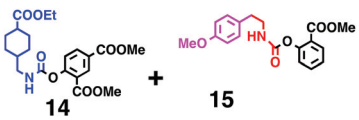	0 °C	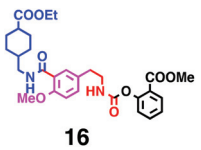	 17 20 °C	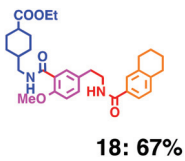 18: 67%
5	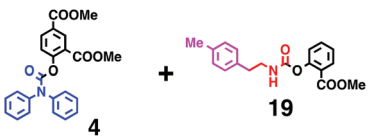	0 °C	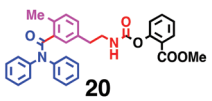	 21 20 °C	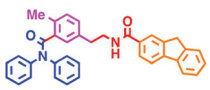 22: 62%
6	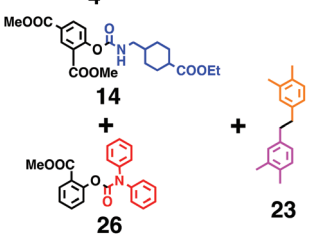	0 °C	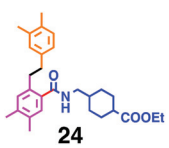	20 °C	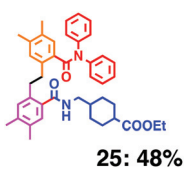 25: 48%

ated very slowly (in around half a day) from carbamates (**42** or **44**) containing *para*-monosubstituted phenol at 20 °C. As described above, these combined reactions enable temporally controlled generation of highly reactive electrophiles (blue, red, and green), which react rapidly with one equivalent of the target aromatic compounds (pink, orange, and brown).

The desired compounds were obtained in relatively good yields (**43**: 56%; **45**: 53%) (these yields are three-step yields, so the average yield in reaction (a) is 82% and that in reaction (b) is 81%, respectively). Thus, we can control the unmasking reaction rates and the time of generation of highly reactive electrophiles.

Although the third electrophilic reaction was intramolecular and the third component (**5**) was added after the first S_EAr reaction between the first and second components was completed, three components were combined into a single aromatic molecule in one pot with high regioselective formation of three bonds.

This reaction design is, therefore, a potential avenue to realize ultimate multi-component electrophilic aromatic substitution reactions (as shown in Chart 1(b)).

Conclusion

Tuning of the leaving group ability of phenolate derivatives from carbamates (**1a–1d**) and ester (**1e**) enables temporal control of the generation of multiple electrophiles (unmasking) simply by appropriate selection of the reaction temperature, so that the autonomous sequential electrophilic aromatic substitution reactions can proceed in one pot. This chemistry thus allows individual functionalization of several different aromatic moieties in one molecule by means of multiple electrophilic aromatic substitution reactions, affording complex aromatic assemblies in one pot. While the number of bonds that can be formed is unlimited in theory, in the present work,

Table 2 Two-step buildup of complexity of aromatic molecules by acylation and amidation

Entry	Substrates	Reaction temperature 1	Intermediate	Reaction temperature 2 and 3rd substrate	Final product
1	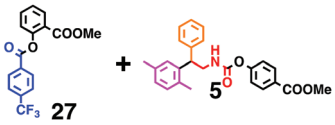 **27** + **5**	0 °C	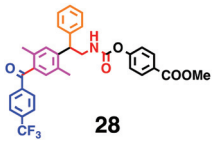 **28**	20 °C	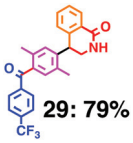 **29: 79%**
2	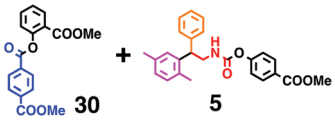 **30** + **5**	0 °C	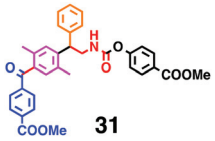 **31**	20 °C	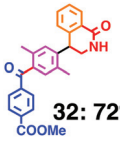 **32: 72%**
3	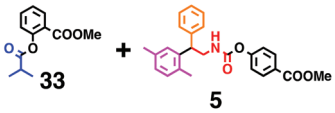 **33** + **5**	0 °C	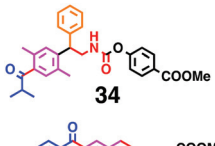 **34**	20 °C	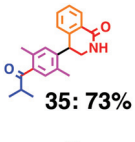 **35: 73%**
4	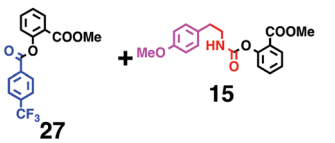 **27** + **15**	0 °C	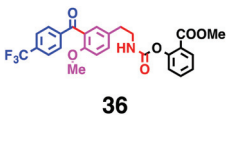 **36**	 **37** 20 °C	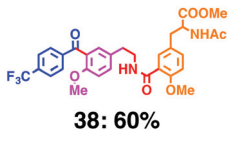 **38: 60%**
5	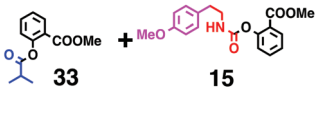 **33** + **15**	0 °C	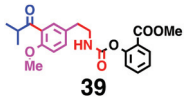 **39**	 **40** 20 °C	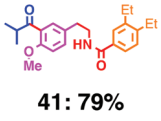 **41: 79%**

we demonstrated autonomous formation of up to three bonds in one pot, and we realized one example of the three-component reaction to make two amide bonds. In order to use this system for practical reactions applicable to the synthesis of libraries of compounds, it will be necessary to reduce the amount of acid and to design sophisticated leaving group systems. Nevertheless, in this work, we have demonstrated the conceptual validity of a one-pot build-up of a complex aromatic molecule from multiple starting components, ultimately leading to multi-component electrophilic aromatic substitution reactions (Chart 1(b)).

Experimental procedure

General procedures

The melting points were determined with a Yanaco micro melting point apparatus without correction. ^{1}H- (400 MHz) and ^{13}C- (100 MHz) NMR spectra were recorded on a Bruker Avance 400. Chemical shifts were calibrated with tetramethylsilane as an internal standard or with the solvent peak, and are shown in ppm (δ) values, and coupling constants are shown in hertz (Hz). The following abbreviations are used: s = singlet, d = doublet, t = triplet, q = quartet, dd = double doublet, dt = double triplet, dq = double quartet, h = hextet, m = multiplet, and brs = broad singlet. Electron spray ionization time-of-flight mass spectra (ESI-TOF MS) were recorded on a Bruker micrOTOF-05 to give high-resolution mass spectra (HRMS). All reagents were commercially available and used without further purification, unless otherwise noted. Flash column chromatography was carried out on silica gel (silica gel (40–63 μm)). The combustion analyses were carried out in the microanalytical laboratory of this department.

Preparation of substrates

Preparation of dimethyl 4-((diphenylcarbamoyl)oxy)isophthalate (4). To a solution of dimethyl 4-hydroxyisophthalate (698.2 mg, 3.32 mmol) in iPr_2NEt (0.65 mL), diphenylcarbamic chloride (717.8 mg, 3.10 mmol) was added at rt. The whole mixture was stirred for 13 hours at rt. After the reaction completed, 2 M aqueous solution of HCl (40 mL) was added and then extracted with CH_2Cl_2 (40 mL × 3). The organic phase was washed with brine (40 mL), dried over Na_2SO_4, and the solvent was evaporated under reduced pressure to give a residue, which was flash column-chromatographed on silica-gel (eluent: EtOAc/*n*-hexane = 1/2) to afford dimethyl 4-((diphenylcarbamoyl)oxy)isophthalate (**4**) (1223.8 mg, 3.02 mmol, 97%) as a colorless solid. Mp. 158.9–159.7 °C (colorless needles, recrystallized from CH_2Cl_2/*n*-hexane). ^{1}H-NMR ($CDCl_3$, 400 MHz) δ (ppm): 8.649 (1H, d, J = 2.0 Hz), 8.173 (1H, dd, J = 8.4, 2.0 Hz), 7.448–7.352 (8H, m), 7.265–7.197 (3H, m), 3.933 (3H, s), 3.920 (3H, s). ^{13}C-NMR ($CDCl_3$, 100 MHz) δ (ppm): 166.10, 164.86, 154.82, 152.75, 142.75, 135.13, 133.67, 129.60, 128.27, 127.23 (br), 124.67, 124.56, 52.98, 52.92. HRMS (ESI-TOF, $[M + Na]^+$): Calcd for $C_{23}H_{19}NNaO_6^+$: 428.1105.

Found: 428.1105. Anal. Calcd for $C_{23}H_{19}NO_6$: C, 68.14; H, 4.72; N, 3.46. Found: C, 67.79; H, 4.90; N, 3.32.

Preparation of methyl 4-(((2-(2,5-dimethylphenyl)-2-phenylethyl)-carbamoyl)oxy)benzoate (5). To a solution of *para*-xylene (5 mL) in TfOH (10 mL), 2-amino-1-phenylethanol (1011.2 mg, 7.37 mmol) was added at 0 °C. The whole mixture was warmed up from 0 °C to 20 °C, and stirred for 2 hours. After the reaction completed, the whole mixture was poured into ice-water and 2 M aqueous solution of NaOH (50 mL) was added. This reaction mixture was extracted with CH_2Cl_2 (30 mL × 4). The organic phase was washed with brine (30 mL), dried over Na_2SO_4, and the solvent was evaporated under reduced pressure to give a yellow crude (1784.3 mg). Then this crude was added to the solution of dimethyl 4,4′-(carbonylbis(oxy))dibenzoate (2109.0 mg, 6.39 mmol) in THF (20 mL) at rt. The whole mixture was stirred for 4 hours at rt. After the reaction completed, 2 M aqueous solution of NaOH (40 mL) was added and then extracted with CH_2Cl_2 (30 mL × 4). The organic phase was washed with brine (30 mL), dried over Na_2SO_4, and the solvent was evaporated under reduced pressure to give a residue, which was column-chromatographed on silica-gel (eluent: EtOAc/*n*-hexane = 2/3) to afford methyl 4-(((2-(2,5-dimethylphenyl)-2-phenylethyl)carbamoyl)-oxy)benzoate (**5**) (222.0 mg, 4.99 mmol, 68% in two steps) as a colorless amorphous material.

^{1}H-NMR ($CDCl_3$, 400 MHz) δ (ppm): 8.011 (2H, d, J = 8.4 Hz), 7.297 (2H, t, J = 7.6 Hz), 7.230–7.194 (3H, m), 7.135 (2H, td, J = 8.8, 2.0 Hz), 7.080–7.047 (2H, m), 6.990–6.971 (1H, m), 5.190–4.866 (1H, m), 4.419 (1H, t, J = 8.0 Hz), 3.878 (5H, m), 2.333 (3H, s), 2.229 (3H, s). ^{13}C-NMR ($CDCl_3$, 100 MHz) δ (ppm): 166.92, 155.23, 154.20, 141.77, 139.50, 136.17, 134.34, 131.55, 131.45, 129.23, 128.79, 128.08, 127.54, 127.31, 121.77, 52.60, 47.24, 46.00, 21.78, 19.80. HRMS (ESI-TOF, $[M + Na]^+$): Calcd for $C_{25}H_{25}NNaO_4^+$: 426.1676. Found: 426.1652. Anal. Calcd for $C_{25}H_{25}NO_4 + 0.2H_2O$: C, 73.76; H, 6.29; N, 3.44. Found: C, 73.46; H, 6.02; N, 3.25.

Preparation of dimethyl 4-((((4-(ethoxycarbonyl)cyclohexyl)-methyl)-carbamoyl)oxy)isophthalate (14). To a solution of $SOCl_2$ (0.5 mL, 6.9 mmol) in EtOH (20 mL) was added 4-(aminomethyl)cyclohexane-1-carboxylic acid (847.2 mg, 5.39 mmol) at 0 °C, and the whole mixture was stirred for 30 minutes at rt, then for 1 hour at reflux. After the reaction completed, the mixture was poured into ice-water and quenched with 2 M aqueous solution of NaOH (50 mL). Then, EtOAc (100 mL) was added and the mixture was washed with 2 M aqueous solution of NaOH (50 mL × 2). The organic phase was washed with brine (30 mL), dried over Na_2SO_4, and the solvent was evaporated under reduced pressure to give a crude (947.6 mg). To a solution of tetramethyl 4,4′-(carbonylbis(oxy))diisophthalate (1362.0 mg, 3.05 mmol) in THF (8.0 mL), the crude (947.6 mg) in THF (2.0 mL) was added at 0 °C. The whole mixture was stirred for 10 minutes at 0 °C. The reaction mixture was purified by column-chromatography on silica gel (eluent: EtOAc/*n*-hexane = 2/3) to afford dimethyl 4-((((4-(ethoxycarbonyl)cyclohexyl)methyl)carbamoyl)oxy)isophthalate (**14**) (947.6 mg, 2.25 mmol, 42% in two steps) as a colorless solid. Mp. 122.3–123.2 °C (colorless needles, recrystallized from CH_2Cl_2/*n*-hexane). ^{1}H-NMR ($CDCl_3$, 400 MHz) δ (ppm) (presence of two amide conformers): 8.646–8.607 (1H, m), 8.186 (1H, dd, J = 8.6, 2.0 Hz), 7.236 (1H, d, J = 8.4 Hz), 5.413 (0.89H, t, J = 13.2 Hz), 5.085 (0.11H, brs), 4.121 (2H, q, J = 6.8 Hz), 3.930 (3H, s), 3.883 (3H, s), 3.238 (0.24H, t, J = 6.4 Hz), 3.129 (1.84H, t, J = 6.4 Hz), 2.238 (1H, tt, J = 12.1, 3.6 Hz), 2.051–2.017 (2H, m), 1.929–1.850 (2H, m), 1.605–1.390 (3H, m), 1.250 (3H, t, J = 7.2 Hz), 1.015 (2H, qd, J = 13.2, 3.2 Hz). ^{13}C-NMR ($CDCl_3$, 100 MHz) δ (ppm): 176.33, 166.10, 165.05, 154.57, 154.35, 134.99, 133.49, 127.97, 124.78, 124.65, 60.69, 52.87, 52.81, 47.81, 43.72, 38.00, 30.06, 28.88, 14.70. HRMS (ESI-TOF, $[M + Na]^+$): Calcd for $C_{21}H_{27}NNaO_8^+$: 444.16129. Found: 444.1619. Anal. Calcd for $C_{21}H_{27}NO_8$: C, 59.85; H, 6.46; N, 3.32. Found: C, 59.73; H, 6.35; N, 3.29.

Preparation of methyl 2-((diphenylcarbamoyl)oxy)benzoate (26). To a solution of triphosgene (300.3 mg, 1.01 mmol) in CH_2Cl_2 (3.0 mL) were added a solution of diphenylamine (364.4 mg, 2.15 mmol) in CH_2Cl_2 (4.0 mL) and dry pyridine (1.0 mL) at 0 °C. The resulting mixture was stirred at 0 °C for 15 min and at rt for an additional 17.5 h. The reaction was quenched with 2 M aqueous solution of HCl (20 mL). The reaction mixture was extracted with CH_2Cl_2 (20 mL × 5). The organic phase was washed with brine (20 mL), dried over Na_2SO_4, and the solvent was evaporated to give the crude isocyanate (498.9 mg). To a solution of methyl 2-hydroxybenzoate (518.3 mg, 3.41 mmol), pyridine (3.0 mL) and iPr_2NEt (0.5 mL, 2.87 mmol), a solution of the above crude isocyanate (498.9 mg) in CH_2Cl_2 (4.0 mL) was added at rt. The whole mixture was stirred for 3 h at rt. The crude reaction mixture was purified by column-chromatography on silica gel (eluent: EtOAc/*n*-hexane = 1/2) to afford methyl 2-((diphenylcarbamoyl) oxy)benzoate (**26**) (636.2 mg, 1.83 mmol, 85%) as a colorless solid. Mp. 82.6–84.9 °C (colorless needles, recrystallized from CH_2Cl_2/*n*-hexane). ^{1}H-NMR ($CDCl_3$, 400 MHz) δ (ppm): 7.976 (1H, d, J = 7.6 Hz), 7.519–7.340 (9H, m), 7.277–7.118 (4H, m), 3.907 (3H, s). ^{13}C-NMR ($CDCl_3$, 100 MHz) δ (ppm): 165.51, 153.24, 151.24, 142.89, 134.05, 131.97, 129.43, 127.51, 126.92, 126.16, 124.22, 124.19, 52.64. HRMS (ESI-TOF, $[M + Na]^+$): Calcd for $C_{21}H_{17}NNaO_4^+$: 370.10498. Found: 370.10432. Anal. Calcd for $C_{21}H_{17}NO_4$: C, 72.61; H, 4.93; N, 4.03. Found: C, 72.77; H, 4.82; N, 4.12.

Preparation of methyl 2-((4-(trifluoromethyl)benzoyl)oxy)-benzoate (27). To a solution of methyl salicylate (15 657.5 mg, 10.3 mmol) in CH_2Cl_2 (20 mL) and iPr_2NEt (9.0 mL), 4-(trifluoromethyl)benzoyl chloride (1823.9 mg, 8.74 mmol) in CH_2Cl_2 (10 mL) was added at 0 °C. The whole mixture was stirred for 40 minutes at 0 °C. The reaction mixture was purified by column-chromatography on silica gel (eluent: EtOAc/*n*-hexane = 1/4) to afford methyl 2-((4-(trifluoromethyl)-benzoyl)oxy)benzoate (**27**) (1142.8 mg, 3.52 mmol, 40%) as a colorless solid. Mp. 68.7–69.2 °C (colorless plates, recrystallized from CH_2Cl_2/*n*-hexane). ^{1}H-NMR ($CDCl_3$, 400 MHz) δ (ppm): 8.339 (2H, d, J = 8.0 Hz), 8.091 (1H, dd, J = 7.8, 1.6 Hz), 7.788 (2H, d, J = 8.0 Hz), 7.627 (1H, td, J = 7.6, 2.0 Hz), 7.383 (1H, td, J = 7.8, 1.2 Hz), 7.252–7.230 (1H, m), 3.750

(3H, s). ^{13}C-NMR ($CDCl_3$, 100 MHz) δ (ppm): 165.33, 164.83, 151.14, 135.55 (q, J = 32 Hz), 134.60, 133.39, 132.60, 131.25, 126.98, 126.22 (q, J = 3 Hz), 124.39, 124.18 (q, J = 271 Hz), 123.73, 52.81. HRMS (ESI-TOF, $[M + Na]^+$): Calcd for $C_{16}H_{11}F_3NaO_4^+$: 347.0507. Found: 347.0496. Anal. Calcd for $C_{16}H_{11}F_3O_4$: C, 59.27; H, 3.42. Found: C, 59.08; H, 3.58.

Preparation of methyl 2-(((4-methoxyphenethyl)carbamoyl)-oxy)benzoate (15). To a solution of dimethyl 2,2′-carbonyldibenzoate (1660.9 mg, 5.03 mmol) in THF (10.0 mL), a solution of 2-(4-methoxyphenyl)ethan-1-amine (776.1 mg, 5.13 mmol) in THF (5.0 mL) was added at rt. The whole mixture was stirred for 1 hour at rt. The reaction mixture was directly purified by column-chromatography on silica gel (eluent: EtOAc/*n*-hexane = 1/1) to afford methyl 2-(((4-methoxyphenethyl)-carbamoyl)oxy)benzoate (**15**) (1630.2 mg, 4.95 mmol, 90%) as a colorless solid.

Mp. 61.2–61.5 °C (colorless cube, recrystallized from CH_2Cl_2/*n*-hexane). ^{1}H-NMR ($CDCl_3$, 400 MHz) δ (ppm) (presence of two amide conformers): 7.954 (1H, dd, J = 8.0, 1.2 Hz), 7.519 (1H, td, J = 7.8, 1.6 Hz), 7.268 (1H, t, J = 7.2 Hz), 7.192–7.128 (3H, m), 5.196 (0.93H, brs), 4.828 (0.14H, brs), 3.845 (3H, s), 3.792 (3H, s), 3.495 (2H, q, 6.8 Hz), 2.839 (3H, t, J = 7.2 Hz). ^{13}C-NMR ($CDCl_3$, 100 MHz) δ (ppm): 165.89, 158.94, 154.94, 151.21, 134.06, 132.01, 131.22, 130.35, 126.11, 124.67, 124.55, 114.70, 55.84, 52.64, 43.32, 35.68. HRMS (ESI-TOF, $[M + Na]^+$): Calcd for $C_{19}H_{18}NNaO_5^+$: 352.1152. Found: 352.1165. Anal. Calcd for $C_{19}H_{18}NO_5$: C, 65.64; H, 5.82; N, 4.25. Found: C, 65.32; H, 5.79; N, 4.11.

Multiple successive electrophile substitution reactions in one pot

Dual amidation in one pot (7) (Table 1, entry 1). To TfOH (2.0 mL), methyl 4-(((2-(2,5-dimethylphenyl)-2-phenylethyl)-carbamoyl)oxy)benzoate **5** (222.5 mg, 0.50 mmol) in CH_2Cl_2 (0.5 mL) was added at 0 °C. Then, dimethyl 4-((diphenylcarbamoyl)oxy)isophthalate **4** (202.9 mg, 0.50 mmol) in CH_2Cl_2 (1.0 mL) was added at 0 °C. The whole mixture was warmed up from 0 °C to 20 °C, and stirred for 12 hours. After the reaction was completed, the whole mixture was poured into ice-water. 2 M aqueous solution of NaOH (50 mL) was added, and this reaction mixture was extracted with CH_2Cl_2 (40 mL × 3). The organic phase was washed with brine (40 mL), dried over Na_2SO_4, and the solvent was evaporated under reduced pressure to give a residue, which was column-chromatographed on silica-gel (eluent: acetone/*n*-hexane = 4/3) to afford 2,5-dimethyl-4-(1-oxo-1,2,3,4-tetrahydroisoquinolin-4-yl)-*N*,*N*-diphenyl-benzamide (**7**) (191.7 mg, 0.43 mmol, 86%) as a colorless solid. Mp. 240.7–241.3 °C (colorless plates, recrystallized from CH_2Cl_2/*n*-hexane). ^{1}H-NMR ($CDCl_3$, 400 MHz) δ (ppm): 8.133 (1H, dd, J = 9.2, 3.6 Hz), 7.394–6.969 (16H, m), 6.831–6.796 (2H, m), 6.760 (1H, s), 5.617 (1H, t, J = 6.0 Hz), 4.550 (1H, t, J = 7.2 Hz), 3.634 (2H, dd, J = 7.8, 2.8 Hz), 3.485 (2H, q, J = 6.4 Hz), 2.749 (2H, t, J = 6.8 Hz), 2.413 (3H, s), 2.342 (3H, s), 2.220 (3H, s). ^{13}C-NMR ($CDCl_3$, 100 MHz) δ (ppm): 171.33, 166.81, 143.51, 141.94, 139.49, 136.06, 133.96, 133.79, 132.91, 130.88, 130.66, 129.63, 129.45, 128.58, 127.89, 127.74, 127.49, 127.03, 46.13, 40.50, 19.81, 19.58. HRMS (ESI-TOF, $[M + Na]^+$): Calcd for $C_{30}H_{26}N_2NaO_2^+$: 469.1886. Found: 469.1876. Anal. Calcd for $C_{30}H_{26}N_2O_2$ + 0.2H_2O: C, 80.05; H, 5.91; N, 6.22. Found: C, 80.13; H, 6.17; N, 6.07.

Three-component dual amidation reactions (25) (Table 1, entry 6). To a solution of 1,2-bis(3,4-dimethylphenyl)ethane **14** (120.3 mg, 0.51 mmol), dimethyl 4-((((4-(ethoxycarbonyl)-cyclohexyl)methyl)carbamoyl)oxy)isophthalate **23** (210.8 mg, 0.50 mmol) and methyl 2-((diphenylcarbamoyl)oxy)benzoate **26** (175.9 mg, 0.51 mmol) in CH_2Cl_2 (1.0 mL), TfOH (2.0 mL) was added at 0 °C. The whole mixture was stirred for 15 minutes. Then, the whole mixture was warmed up from 0 °C to 20 °C, and stirred for 1 hour. After the reaction completed, the whole mixture was poured into ice-water and 2 M aqueous solution of NaOH (30 mL) was added. This reaction mixture was extracted with CH_2Cl_2 (40 mL × 3). The organic phase was washed with brine (40 mL), dried over Na_2SO_4, and the solvent was evaporated under reduced pressure to give a residue, which was column-chromatographed on silica-gel (eluent: EtOAc/*n*-hexane = 1/2) to afford ethyl 4-((2-(2-(diphenylcarbamoyl)-4,5-dimethylphenethyl)-4,5-dimethylbenzamido)-methyl)cyclohexane-1-carboxylate **25** (155.3 mg, 0.24 mmol, 48%) as a colorless oil. ^{1}H-NMR ($CDCl_3$, 400 MHz) δ (ppm) (presence of two amide conformers): 7.181–6.792 (14H, m), 6.101–6.032 (1H, m), 4.028 (2H, q, J = 7.2 Hz), 3.103 (2H, t, J = 6.4 Hz), 2.994–2.865 (5H, m), 2.157–2.122 (6H, m), 2.053 (3H, s), 1.954 (3H, m), 1.873–1.692 (5H, m), 1.411–1.337 (1H, m), 1.267 (2H, qd, J = 13.2, 3.2 Hz), 1.162 (3H, t, J = 7.2 Hz), 0.856 (2H, qd, J = 12.8, 3.6 Hz). ^{13}C-NMR ($CDCl_3$, 100 MHz) δ (ppm): 175.96, 175.88, 171.14, 171.10, 170.84, 170.34, 143.44, 143.34, 138.38, 138.03, 137.86, 137.80, 137.47, 137.25, 136.92, 135.70, 134.68, 134.33, 134.25, 133.55, 133.52, 133.33, 133.25, 132.55, 131.52, 131.06, 130.88, 130.13, 129.35, 129.05, 128.92, 128.53, 127.42, 126.90, 126.75, 126.31, 126.28, 60.39, 60.13, 53.45, 45.66, 45.45, 43.32, 43.28, 37.36, 37.18, 35.24, 34.99, 34.93, 34.78, 29.97, 29.86, 28.49, 28.44, 21.04, 19.90, 19.64, 19.57, 19.19, 19.03, 16.51, 14.25. HRMS (ESI-TOF, $[M + Na]^+$): Calcd for $C_{40}H_{37}N_3NaO_3^+$: 630.2727. Found: 630.2731. Anal. Calcd for $C_{40}H_{37}N_3O_3$ + 0.6 CH_2Cl_2: C, 74.03; H, 5.85; N, 6.38. Found: C, 74.06; H, 6.07; N, 6.18.

Sequential aromatic acylation–amidation reaction 29 (Table 2, entry 1). To a mixture of TfOH (2.0 mL), methyl 4-(((2-(2,5-dimethylphenyl)-2-phenylethyl)carbamoyl)oxy)benzoate **5** (441.8 mg, 1.1 mmol) in CH_2Cl_2 (2.0 mL) was slowly added at 0 °C. Then, methyl 2-((4-(trifluoromethyl)benzoyl)oxy)-benzoate **27** (359.4 mg, 1.11 mmol) was added at 0 °C. The whole mixture was warmed up from 0 °C to 20 °C, and stirred for 15 hours. After the reaction was completed, the whole mixture was poured into ice-water. This reaction mixture was extracted with CH_2Cl_2 (30 mL × 4). The organic phase was washed with brine (40 mL), dried over Na_2SO_4, and the solvent was evaporated under reduced pressure to give a residue, which was column-chromatographed on silica-gel (eluent: EtOAc/*n*-hexane = 1/1) to afford 4-(2,5-dimethyl-4-(4-(trifluoromethyl)benzoyl)-phenyl)-3,4-dihydroisoquinolin-1(2*H*)-one (**29**) (367.5 mg, 0.87 mmol, 79%) as a colorless solid.

Mp. 237.2–237.9 °C (colorless needles, recrystallized from EtOAc). ^{1}H-NMR (DMSO-d_6, 400 MHz) δ (ppm): 8.002–7.888 (6H, m), 7.458 (2H, td, J = 24.5, 7.2 Hz), 7.276 (1H, s), 6.973 (1H, d, J = 7.2 Hz), 6.779 (1H, s), 4.619 (1H, t, J = 6.0 Hz), 3.699–3.524 (2H, m), 2.394 (3H, s), 2.102 (3H, s). ^{13}C-NMR (DMSO-d_6, 100 MHz) δ (ppm): 196.52, 164.35, 142.46, 141.00, 140.68, 135.64, 134.06, 133.65, 132.53 (q, J = 32 Hz), 132.20, 131.02, 130.81, 130.32, 129.86, 127.46, 127.27, 127.23, 125.79 (q, J = 4 Hz), 123.76 (q, J = 271 Hz), 44.44, 39.16, 19.43, 18.68. HRMS (ESI-TOF, $[M + Na]^+$): Calcd for $C_{25}H_{20}F_3NNaO_2^+$: 446.1338. Found: 446.1334. Anal. Calcd for $C_{25}H_{20}F_3NO_2$ + 0.8 H_2O: C, 68.58; H, 4.97; N, 3.20. Found: C, 68.74; H, 5.04; N, 3.09.

Formation of three bonds in a one-pot reaction 43 (Fig. 8, reaction (a)). To TfOH (2.0 mL), methyl 2-(((4-methoxyphenethyl)carbamoyl)oxy)benzoate **15** (166.1 mg, 0.50 mmol) was added at 0 °C. Then, methyl 2-((4-(trifluoromethyl)benzoyl)oxy)-benzoate **27** (164.0 mg, 0.51 mmol) was added at 0 °C. The whole mixture was stirred for 15 minutes. Then, methyl 4-(((2-(2,5-dimethylphenyl)-2-phenylethyl)carbamoyl)oxy)benzoate **5** (230.3 mg, 0.52 mmol) in CH_2Cl_2 (2.0 mL) was added at 0 °C. The whole mixture was warmed up from 0 °C to 20 °C, and stirred for 15 hours. After the reaction was completed, the whole mixture was poured into ice-water and 2 M aqueous solution of NaOH (30 mL) was added. This reaction mixture was extracted with CH_2Cl_2 (40 mL × 3). The organic phase was washed with brine (40 mL), dried over Na_2SO_4, and the solvent was evaporated under reduced pressure to give a residue, which was column-chromatographed on silica-gel (eluent: EtOAc) to afford *N*-(4-methoxy-3-(4-(trifluoromethyl)benzoyl) phenethyl)-2,5-dimethyl-4-(1-oxo-1,2,3,4-tetrahydroisoquinolin-4-yl)benzamide **43** (172.7 mg, 0.29 mmol, 56%) as an amorphous material. ^{1}H-NMR ($CDCl_3$, 400 MHz) δ (ppm): 8.143–8.120 (1H, m), 7.869 (2H, d, J = 8.0 Hz), 7.673 (2H, d, J = 8.4 Hz), 7.424–7.373 (3H, m), 7.301 (1H, d, J = 2.4 Hz), 7.183 (1H, s), 6.961 (1H, d, J = 8.4 Hz), 6.818–6.796 (1H, m), 6.747 (1H, s), 6.608 (1H, brs), 5.956 (1H, t, J = 6.0 Hz), 4.546 (1H, t, J = 7.6 Hz), 3.725–3.630 (7H, m), 2.934 (2H, t, J = 7.6 Hz), 2.327 (3H, s), 2.232 (3H, s). ^{13}C-NMR ($CDCl_3$, 100 MHz) δ (ppm): 195.93, 170.41, 166.80, 156.86, 141.69, 141.30, 140.66, 135.88, 134.54 (q, J = 28 Hz), 134.37, 134.31, 133.62, 133.15, 131.79, 131.52, 131.02, 130.70, 130.35, 129.73, 128.72, 128.56, 127.97, 127.84, 125.79 (q, J = 3 Hz), 124.24 (q, J = 271 Hz), 112.43, 56.20, 46.31, 41.38, 40.56, 35.25, 19.94, 19.67. HRMS (ESI-TOF, $[M + Na]^+$): Calcd for $C_{35}H_{31}F_3N_2NaO_4^+$: 623.2128. Found: 623.2128. Anal. Calcd for $C_{35}H_{31}F_3N_2O_4$ + 0.5 CH_2Cl_2: C, 66.30; H, 5.02; N, 4.36. Found: C, 66.05; H, 5.33; N, 4.35.

Computational methods

We carried out computational studies by using the Gaussian 09 suites of programs.[19] The geometries of the reactants (SM), transition states (TS), and products (PM) for dissociation steps were fully optimized using the CPCM (Complete Polarizable Continuum Model)-B3LYP/6-31+G(d) level.[20] Harmonic vibrational frequency computations characterized the optimized structures. Intrinsic reaction coordinate (IRC) computations[21] of the transition structures verified the reactants, intermediates, and products on the potential energy surface (PES). Bulk solvation effects (self-consistent reaction field, SCRF) were simulated by the CPCM method[22] in trifluoromethanesulfonic acid as a solvent (eps = 77.4,[23] rsolv = 2.5985274,[23] density = 1.696,[24] epsinf = 1.882384 (the value of acetic acid was employed)). Single point energies were calculated with CPCM-M06-2X/6-311++G(d,p) (and some other calculation levels) on the basis of the optimized structures.[25] The zero-point vibrational energy corrections were done without scaling.

Acknowledgements

This work was supported by the University of Tokyo. The computations were performed at the Research Center for Computational Science, Okazaki, Japan. We thank the computational facility for generous allotments of computer time.

Notes and references

1 P. J. Hajduk and J. Greer, *Nat. Rev. Drug Discovery*, 2007, **6**, 211–219.
2 S. L. Schreiber, *Science*, 2000, **287**, 1964–1969.
3 Y. Takayama, T. Yamada, S. Tatekabe and K. Nagasawa, *Chem. Commun.*, 2013, **49**, 6519.
4 (*a*) H. Kheira, P. Li and J. Xu, *J. Mol. Catal. A: Chem.*, 2014, **391**, 168–174; (*b*) X. Zhang, W. T. Teo and P. W. H. Chan, *Org. Lett.*, 2009, **11**, 4990–4993; (*c*) M. Shi, L. Wu and J. Lu, *Tetrahedron*, 2008, **64**, 3315–3321; (*d*) J. A. Kozak, B. O. Patrick and G. R. Dake, *J. Org. Chem.*, 2010, **75**, 8585–8590.
5 (*a*) Y. Zhang, L. Chen and T. Lu, *Adv. Synth. Catal.*, 2011, **353**, 1055–1060; (*b*) R. O. Iakovenko, A. N. Kazakova, V. M. Muzalevskiy, A. Y. Lvanov, I. A. Boyarskaya, A. Chicca, V. Petrucci, J. Gertsch, M. Krasavin, G. L. Starova, A. A. Zolotarev, M. S. Avdontceva, V. G. Nenajdenko and A. V. Vasilyev, *Org. Biomol. Chem.*, 2015, **13**, 8827–8842.
6 (*a*) B. R. Park, S. H. Kim, Y. M. Kim and J. N. Kim, *Tetrahedron Lett.*, 2011, **52**, 1700–1704; (*b*) B. V. Ramulu and G. Satyanarayana, *RSC Adv.*, 2015, **5**, 70972–70976; (*c*) R. Rendy, Y. Zhang, A. McElrea, A. Gomez and D. A. Klumpp, *J. Org. Chem.*, 2004, **69**, 2340–2347.
7 (*a*) F. Sun, M. Zeng, Q. Gu and S. You, *Chem. – Eur. J.*, 2009, **15**, 8709–8712; (*b*) Q. Li, W. Xu, J. Hu, X. Chen, F. Zhang and H. Zheng, *RSC Adv.*, 2014, **4**, 27722–27725; (*c*) S. Wang, L. Han, M. Zeng, F. Sun, W. Zhang and S. You, *Org. Biomol. Chem.*, 2012, **10**, 3202–3209.
8 (*a*) A. Suárez, P. García-García, M. A. Fernández-Rodríguez and R. Sanz, *Adv. Synth. Catal.*, 2014, **356**, 374–382; (*b*) R. Sureshbabu, V. Saravanan, V. Dhayalan and A. K. Mohanakrishnan, *Eur. J. Org. Chem.*, 2011, 922–935; (*c*) L. Bianchi, M. Maccagno, M. Pani, G. Petrillo, C. Scapolla and C. Tavani, *Tetrahedron*, 2015, **71**, 7421–

7435; (*d*) A. Kulkarni, P. Quang and B. Török, *Synthesis*, 2009, 4010–4014.

9 (*a*) J. Liu, T. He and L. Wang, *Tetrahedron*, 2011, **67**, 3420–3426; (*b*) M. Shiri, M. A. Zolfigol and R. Ayazi-Nasrabadi, *Tetrahedron*, 2010, **51**, 264–268; (*c*) J. Xu, J. Xia and Y. Lan, *Synth. Commun.*, 2005, **35**, 2347–2353; (*d*) S. Saito, T. Ohwada and K. Shudo, *J. Am. Chem. Soc.*, 1995, **117**, 11081–11084; (*e*) G. A. Olah, G. Rasul, C. York and G. K. S. Prakash, *J. Am. Chem. Soc.*, 1995, **117**, 1121–11214; (*f*) P. Thirupathi and S. S. Kim, *J. Org. Chem.*, 2009, **74**, 7755–7761; (*g*) C. Huo, C. Sun, C. Wang, X. Jia and W. Chang, *ACS Sustainable Chem. Eng.*, 2013, **1**, 549–553; (*h*) C. Huo, C. Wang, C. Sun, X. Jia, X. Wang, W. Chang and M. Wu, *Adv. Synth. Catal.*, 2013, **355**, 1911–1916.

10 (*a*) H. Ishida, H. Nukaya, K. Tsuji, H. Zenda and T. Kosuge, *Chem. Pharm. Bull.*, 1992, **40**, 308–313; (*b*) H. Naeimi and S. S. Brojerdi, *Polycyclic Aromat. Compd.*, 2014, **34**, 504–517; (*c*) A. P. Krapcho, Z. Getahun and K. J. Avery Jr., *Synth. Commun.*, 1990, **24**, 2139–2146; (*d*) G. A. Guerrero-Vásquez, C. K. Z. Andrade, J. M. G. Molinillo and F. A. Macías, *Eur. J. Org. Chem.*, 2013, 6175–6180; (*e*) R. Huot and P. Brassard, *Can. J. Chem.*, 1974, **52**, 838–842.

11 (*a*) L. Bianchi, M. Maccagno, M. Pani, G. Petrillo, C. Scapolla and C. Tavani, *Tetrahedron*, 2015, **71**, 7421–7435; (*b*) G. Gangadhararao, A. Uruvakilli and K. C. K. Swamy, *Org. Lett.*, 2014, **16**, 6060–6063; (*c*) L. Hao, Y. Pan, T. Wang, M. Lin, L. Chen and Z. Zhan, *Adv. Synth. Catal.*, 2010, **352**, 3215–3222; (*d*) S. Sarkar, K. Bera and U. Jana, *Tetrahedron Lett.*, 2014, **55**, 6188–6192; (*e*) X. Xie, X. Du, Y. Chen and Y. Liu, *J. Org. Chem.*, 2011, **76**, 9175–9181; (*f*) A. C. Silvanus, S. J. Heffernan, D. J. Liptrot, G. Kociok-Köhn, B. I. Andrews and D. R. Carbery, *Org. Lett.*, 2009, **11**, 1175–1178; (*g*) H. Li, R. Guillot and V. Gandon, *J. Org. Chem.*, 2010, **75**, 8435–8449; (*h*) K. Fuchibe, H. Jyono, M. Fujiwara, T. Kudo, M. Yokota and J. Ichikawa, *Chem. – Eur. J.*, 2011, **17**, 12175–12185.

12 Up to the present, masked (blocked) electrophiles have mainly been limited to masked (blocked) isocyanates. For a review of masked (blocked) isocyanates, see: E. Delebecq, J. Pascault, B. Boutevin and F. Ganachaud, *Chem. Rev.*, 2013, **113**, 80–118. Recent studies on application masked isocyanates to synthetic organic chemistry: (*a*) M. Hutchby, C. E. Houlden, J. G. Ford, S. N. G. Tyler, M. R. Gagné, G. C. Lloyd-Jones and K. I. Booker-Milburn, *Angew. Chem., Int. Ed.*, 2009, **48**, 8721–8724; (*b*) C. Clavette, J. V. Rocan and A. M. Beauchemin, *Angew. Chem., Int. Ed.*, 2013, **52**, 12705–12708; (*c*) H. Ying, Y. Zhang and J. Cheng, *Nat. Commun.*, 2014, **5**, 3218; (*d*) Y. Wei, J. Liu, S. Lin, H. Ding, F. Liang and B. Zhao, *Org. Lett.*, 2010, **12**, 4220–4223; (*e*) C. Spyropoulos and C. G. Kokotos, *J. Org. Chem.*, 2014, **79**, 4477–4483; (*f*) S. Adachi, M. Onozuka, Y. Yoshida, M. Ide, Y. Saikawa and M. Nakata, *Org. Lett.*, 2014, **16**, 358–361; (*g*) E. K. Raja, S. O. N. Lill and D. A. Klumpp, *Chem. Commun.*, 2012, **48**, 8141–8143; (*h*) H. Kurouchi, K. Kawamoto, H. Sugimoto, S. Nakamura, Y. Otani and T. Ohwada, *J. Org. Chem.*, 2012, **77**, 9313–9328.

13 (*a*) A. Sumita, H. Kurouchi, Y. Otani and T. Ohwada, *Chem. – Asian J.*, 2014, **9**, 2995–3004; (*b*) H. Kurouchi, A. Sumita, Y. Otani and T. Ohwada, *Chem. – Eur. J.*, 2014, **20**, 8682–8690.

14 In recent years, several reports have shown that isocyanates are useful chemical species to form aromatic amides. (*a*) G. Schäfer, C. Matthey and J. W. Bode, *Angew. Chem., Int. Ed.*, 2012, **57**, 9173–9175; (*b*) G. Schäfer and J. W. Bode, *Org. Lett.*, 2014, **16**, 1526–1529 and ref. 12*h*.

15 P. Gund, *J. Chem. Educ.*, 1972, **49**, 10–103.

16 J. P. Hwang, G. K. S. Prakash and G. A. Olah, *Tetrahedron*, 2000, **56**, 7199–7203.

17 M. Kozelj and A. Petric, *Synlett*, 2007, 1699–1702.

18 A. Kethe, A. F. Tracy and D. A. Klumpp, *Org. Biomol. Chem.*, 2011, **9**, 4545.

19 M. J. Frisch, G. W. Trucks, H. B. Schlegel, G. E. Scuseria, M. A. Robb, J. R. Cheeseman, G. Scalmani, V. Barone, B. Mennucci, G. A. Petersson, H. Nakatsuji, M. Caricato, X. Li, H. P. Hratchian, A. F. Izmaylov, J. Bloino, G. Zheng, J. L. Sonnenberg, M. Hada, M. Ehara, K. Toyota, R. Fukuda, J. Hasegawa, M. Ishida, T. Nakajima, Y. Honda, O. Kitao, H. Nakai, T. Vreven, J. A. Montgomery Jr., J. E. Peralta, F. Ogliaro, M. Bearpark, J. J. Heyd, E. Brothers, K. N. Kudin, V. N. Staroverov, R. Kobayashi, J. Normand, K. Raghavachari, A. Rendell, J. C. Burant, S. S. Iyengar, J. Tomasi, M. Cossi, N. Rega, N. J. Millam, M. Klene, J. E. Knox, J. B. Cross, V. Bakken, C. Adamo, J. Jaramillo, R. Gomperts, R. E. Stratmann, O. Yazyev, A. J. Austin, R. Cammi, C. Pomelli, J. W. Ochterski, R. L. Martin, K. Morokuma, V. G. Zakrzewski, G. A. Voth, P. Salvador, J. J. Dannenberg, S. Dapprich, A. D. Daniels, Ö. Farkas, J. B. Foresman, J. V. Ortiz, J. Cioslowski and D. J. Fox, *Gaussian 09*, Gaussian, Inc., Wallingford, CT, 2009.

20 A. D. Becke, *J. Chem. Phys.*, 1993, **98**, 5648.

21 K. Fukui, *Acc. Chem. Res.*, 1981, **14**, 363–368.

22 (*a*) V. Barone and M. Cossi, *J. Phys. Chem. A*, 1998, **102**, 1995–2001; (*b*) M. Cossi, N. Rega, G. Scalmani and V. Barone, *J. Comput. Chem.*, 2003, **24**, 669–681.

23 A. L. Lira, M. Zolotukhin, L. Fomina and S. Fomine, *J. Phys. Chem. A*, 2007, **111**, 13606–13610.

24 R. Corkum and J. Milne, *Can. J. Chem.*, 1978, **56**, 1832–1835.

25 Y. Zhao and D. G. Truhlar, *Theor. Chem. Acc.*, 2008, **120**, 215–241.